Observation of wavelength-switchable solitons in an all-polarization-maintaining erbium-doped fiber cavity based on graphene saturable absorber reflector*

Kuo Meng(孟阔), Lian-Qing Zhu(祝连庆)†, and Fei Luo(骆飞)

Beijing Engineering Research Center of Optoelectronics Information and Instrument, Beijing Key Laboratory of Optoelectronic Measurement Technology, Beijing Laboratory for Biomedical Detection Technology and Instrument, Beijing Information Science and Technology University, Beijing 100192, *China*

(Received 1 July 2016; revised manuscript received 9 September 2016; published online 30 November 2016)

We present the generation of wavelength-switchable single-polarization solitons in an all-polarization-maintaining erbium-doped fiber laser mode-locked by a graphene saturable absorber. Ultrashort pulses centered at the wavelength of 1531.6 nm with the duration of 816 fs and centered at the wavelength of 1557.8 nm with the duration of 402 fs are separately obtained from the same fiber laser cavity. The cavity loss adjusted by the gold reflector plays a crucial role in wavelength switching.

Keywords: fiber laser, mode-locked, single-polarization, graphene saturable absorber

PACS: 42.55.Wd, 42.60.Fc **DOI:** 10.1088/1674-1056/26/1/014205

1. Introduction

Fiber lasers serve as lightwave sources for the pulsed electromagnetic energy[1–4] and have a large variety of applications, ranging from small-scale problems such as precision metrologies and ocular surgeries to large-scale problems such as optical communication systems and nuclear fusion. In particular, the precision metrology applications in sensors[5] and optical frequency combs[6] in the C (1530–1565 nm) and L (1565–1625 nm) bands promote the development of the mode-locked fiber laser. Since Mollenauer and Stolen found soliton laser near the wavelength of 1.5 μm in fiber laser in 1983,[7] many researchers have joined in the field and promoted continuously the performance of the mode-locked fiber laser including lifting output power[8,9] and compressing pulse-width.[10,11] Meanwhile, the mode-locked fiber lasers focusing at wavelength modulation have also been studied in depth as an important research orientation. As early as in 1994, wavelength switching in mode-locked fiber laser was realized by pump-diode and selected by Bragg gratings.[12] However, Bragg grating has the drawbacks of restricting the spectral width and suppressing the pulse-width compression. The wavelength-tunable mode-locked laser with an intracavity fiber Fabry–Perot filter[13] still faces the same problem. In the last decade, the research[14,15] also demonstrated that the cavity filtering effect induced by the birefringence in the laser cavity makes the wavelength of the mode-locked laser tunable or switchable. In the method, phase- and intensity-dependent cavity loss adjusted by polarization controllers can be operated, and wavelength-switchable mode-locked solitons can be activated. Actually, the amplified spontaneous emission (ASE) of the erbium-doped fiber always shows spectral humps between around $\sim$ 1532 nm and $\sim$ 1558 nm rather than other wavelength bands in the continuous wave and mode-locked operations by some ways.[16–18] It can be ascribed to the modulation of cavity gain and loss between the two wavelengths.

Recently, single-wavelength all-polarization-maintaining (all-PM) mode-locked fiber lasers have been widely reported using carbon nanotube,[19] grapheme,[20] grapheme oxide[21] as the saturable absorbers and other technologies.[22,23] The predominance is that linear-polarization mode-locked pulses in the all-PM fiber cavity are more robust against environmental variations, and have excellent self-starting and long-term stability. But so far, wavelength-switching mode-locked laser in all-PM fiber cavity has been little reported.

It has been found that new 2D materials such as graphene, molybdenum disulfide (MoS_2),[24] and black phosphorus[25] as the saturable absorbers have advantages compared with the conventional methods. For example, these new materials can be used in mode-locking in a great broadband infrared region, are easy to fabricate, and low in price.

In this paper, we demonstrate for the first time, to the best of our knowledge, wavelength-switchable solitons in an all-PM erbium-doped ring fiber laser by adjusting a gold reflector. A 10-layer graphene film is used as the saturable absorber, and stable passive mode-locking operation is achieved by adhering the graphene film to the gold reflector in the cavity. Wavelength switching between 1531.6 nm and 1557.8 nm can be conveniently obtained in mode-locking.

*Project supported by the Program for Changjiang Scholars and Innovative Research Team in University, China (Grant No. PCSIRT: 1212), the Key Grant Science and Technology Planning Project of Beijing, China (Grant Nos. PXM2013_014224_000077 and PXM2012_014224_000019), and the Science and Technology Planning Project of Beijing Municipal Commission of Education, China (Grant No. KM201611232008).

†Corresponding author. E-mail: zhulianqing@sina.com

© 2017 Chinese Physical Society and IOP Publishing Ltd

2. Experimental setup and methodology

The experimental setup of the all-PM mode-locked fiber laser is illustrated in Fig. 1. The ring cavity consists of a Panda-type PM erbium-doped fiber, a 980/1550 PM wavelength division multiplexer (WDM), a PM-coupler with a 30% output, a PM-circulator, and a 10-layer graphene saturable absorber adhering to a gold-plating reflector (graphene saturable absorber mirror (GSAM) for short). A 976 nm laser diode with the maximum power of 750 mW is used as the pump laser. The absorption coefficient of the PM Er-doped fiber (Nufern, PM-ESF-7/125) is ~ 24.0 dB/m at the wavelength of 976 nm. A three-port PM-circulator (NOVAWAVE) with 1.2 dB insertion loss between ports is employed to assure the anticlockwise propagation of the laser and incorporate the GSAM into the cavity. Port 2 of the PM-circulator consists of a 2.3 mm-length protuberant fiber rod with the diameter of 1.8 mm, the end face of which is polished with the angle of 8° for light anti-reflection (Fig. 1). The laser near 1.5 μm emitted from port 2 of the PM-circulator is close to collimated. The GSAM is loaded into a two-dimensional accurate adjusting mount, and placed adjacent to the cross section of port 2 for coupling most light into the cavity. The total length of the cavity is ~ 3.3 m, which consists of two types of fibers: the PM Er-doped fiber (length of 0.8 m used, group velocity dispersion (GVD) at 1550 nm equals to -0.02 ps^2/m) and the passive PM fiber (total length of 2.5 m, GVD at 1550 nm also equals to ~ -0.02 ps^2/m). Thus, the total cavity is an all-anomalous dispersion cavity with a net group delay dispersion of ~ 0.066 ps^2, and the conventional solitons can be activated in it.

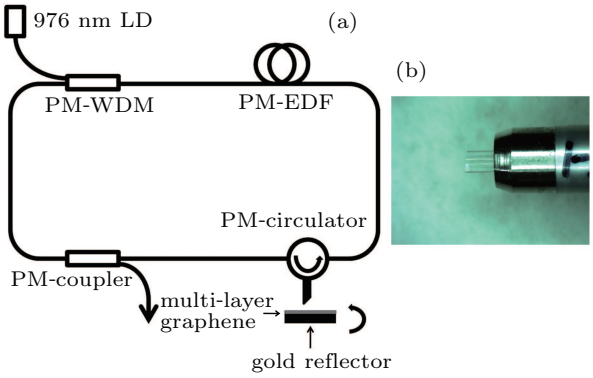


Fig. 1. (a) The schematic setup of all-PM graphene mode-locked erbium-doped fiber laser. (b) The profile of port 2 of the PM-circulator.

The graphene layers used in the experiment are fabricated and deposited on copper foils with the method of chemical vapor deposition (CVD), and then transferred to the gold mirror one-by-one using the polymethylmethacrylate (PMMA) mediator. Because ultrafast pulses are more stable by passively mode-locking using a saturable absorber with higher modulation depth, the multilayer graphene is needed due to its high modulation depth. For example, the measured effective modulation depth of a 21-layer graphene/PMMA composite is 5.5%,[26] higher than the modulation depth ($\sim 0.4\%$) of single-layer grapheme.[27] So, in our experiment, 10-layer GSAM is fabricated, equivalent to 20-layer graphene adhering to the flat window pervious to laser.

In the experiment, wavelength switching between 1531.6 nm and 1557.8 nm of the mode-locked laser can be obtained conveniently by finely tuning the angle of GSAM. The physical origin of wavelength switching can be illuminated using the linear transmission model similar to the model in the previous papers,[17,28,29] which determines the cavity transmission coefficient of the laser cavity. The transmission coefficient can be expressed as

$$|T|^2 = A(\theta) + B(\theta)\cos(\Delta\phi), \tag{1}$$

where $\Delta\phi = \Delta\phi_{\rm EM} + \Delta\phi_{\rm NL} + \Delta\phi_{\rm LB}$ is the net phase delay between the fast and the slow axes of the fiber, $\Delta\phi_{\rm EM}$ is the phase delay induced by the external modulator, $\Delta\phi_{\rm NL}$ is the fiber-induced nonlinear phase change,[30] and $\Delta\phi_{\rm LB} = 2\pi L B_{\rm m}/\lambda$ is the phase delay caused by the linear fiber birefringence.[17] $A(\theta)$ and $B(\theta)$ stand for the intensity loss induced by the angle θ, and θ denotes the reflected angle of the laser by the gold reflector. In the wavelength dynamics of mode-locked laser by the nonlinear polarization rotation (NPR) technique, phase shifts including $\Delta\phi_{\rm EM}$ and $\Delta\phi_{\rm LB}$ are induced by the cavity-birefringence operated by the polarization controllers, which leads to the phase-dependent loss; the intensity modulation involving the terms of A and B is realized by operating the polarization state of the laser by combining the polarization controllers and the polarization dependent isolator, which will lead to the intensity-dependent loss. Different from the NPR technique, in our experiment, $\Delta\phi_{\rm EM}$ is induced by tuning the angle of the gold reflector according to the polarization characteristics of the reflective laser by a metal surface;[31] $\Delta\phi_{\rm LB}$ is constant for the all-PM fiber cavity; the intensity-dependent loss including $A(\theta)$ and $B(\theta)$ can be obtained by modulating the efficiency of the coupling laser into port 2 of the circulator by tuning the angle θ of the gold reflector. In addition, the nonlinear polarization rotation effect may occur in the all-polarization- maintaining cavity and give rise to the mode-locking, but the effect is very weak and can be ignored compared with the graphene saturable absorber reflector. In the experiment, if the graphene saturable absorber reflector is taken away from the cavity, the mode-locking can be observed occasionally, but it is very weak and unstable, and we can ignore it. Therefore, qualitatively, the cavity consisting of the gold reflector and the all-PM fiber has the same functions of realizing both phase-dependent loss and intensity-dependent loss as the NPR technique.

The spectrally and temporally mode-locking performance is simultaneously monitored by an optical spectrum analyzer (Yokogawa, AQ6370D), a 1.0 GHz real-time oscilloscope (LeCroy), a 5.0 GHz InGaAs photo-detector (ThorLabs), an autocorrelator (Femtochrome, FR-103XL), and a 7.5 GHz radio-frequency analyzer (Keysight EXA N9010A). The polarized performance of the output pulses is measured by an extinction ratio meter (Santec PEM-330).

3. Experimental results and discussion

By finely tuning the angle θ of GSAM, the self-started mode-locked pulses are achieved separately at the central wavelengths of 1531.6 nm and 1557.8 nm when the pump power is increased up to 75 mW, as shown in Fig. 2. When mode-locked at 1531.6 nm, the output power is 1.7 mW and the spectrum bandwidth (3 dB) is 2.7 nm at the pump power of 75 mW. When the pump power is 100 mW, the output power increases to 2.4 mW, and the spectrum bandwidth expands to 3.8 nm due to more longitudinal modes induced by the higher nonlinearity of the fiber cavity. However, there are no evident Kelly sidebands of optical spectrum seen from Fig. 2(a). It can be attributed to the longer pulse of mode-locking, which causes the side band amplitude fall off,[32] compared with the pulse-width of mode-locking at the wavelength of 1557.8 nm. When the wavelength of the mode-locked laser is switched to 1557.8 nm, the output power is 3.8 mW and the spectrum bandwidth is 5.4 nm at the pump power of 75 mW. By raising the pump power up to 100 mW, the output power increases to 5.8 mW, and the spectrum bandwidth expands to 7.5 nm. There are clearly visible Kelly sidebands when mode-locked at the wavelength of 1557.8 nm (Fig. 2(b)), just as reported in Refs. [22] and [33]. Specifically, it is found that, with the pump power up to 100 mW, the positions of the sidebands become closer to the peak of the soliton spectrum, and more spectral sidebands appear at both sides of the spectrum, which confirm the theoretical predictions in Ref. [34]. The spectrum data are measured by an optical spectral analyzer with a resolution of 0.02 nm. In repeated experiments, the switched wavelengths of the mode-locked laser output are exactly located at the two wavelengths of 1531.7 nm and 1557.8 nm, no evident wavelength-shifts as the NPR technology.[15,35] It can be ascribed to constant phase delay $\Delta\phi_{\mathrm{LB}}$ induced by the fixed fiber birefringence of the all-PM fiber cavity, different from the polarization controller which can modulate the birefringence of the fiber cavity continuously.

Figure 3 shows the radio-frequency (RF) spectra measured at a span of 50 kHz with 50 Hz resolution bandwidth at 100 mW pump power. The fundamental frequencies are located at 60.6431 MHz and 60.6373 MHz respectively for mode-locking at 1531.6 nm and 1557.8 nm, which shows that there is a tiny disparity between their repetition rates (less than 6 kHz). Both their signal-to-noise ratios are above 70 dB, indicating the same stable single-pulse mode-locking operation. One of their spectra of harmonics at the span of 5 GHz is depicted in the inset of Fig. 3.

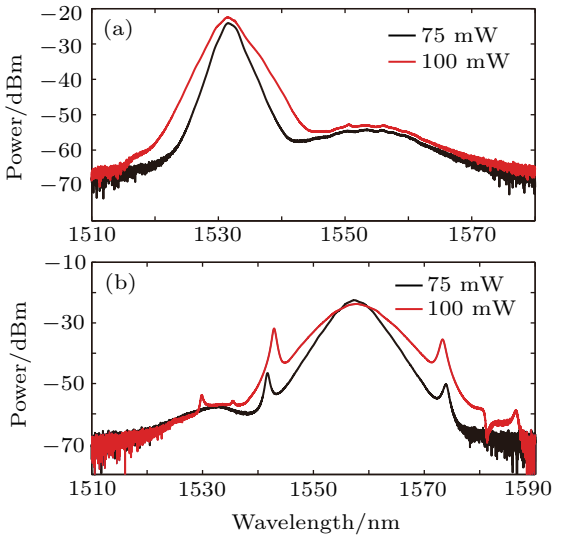


Fig. 2. Optical spectra of all-PM grapheme erbium-doped fiber laser mode-locked at (a) 1531.6 nm and (b) 1557.8 nm with different pump powers.

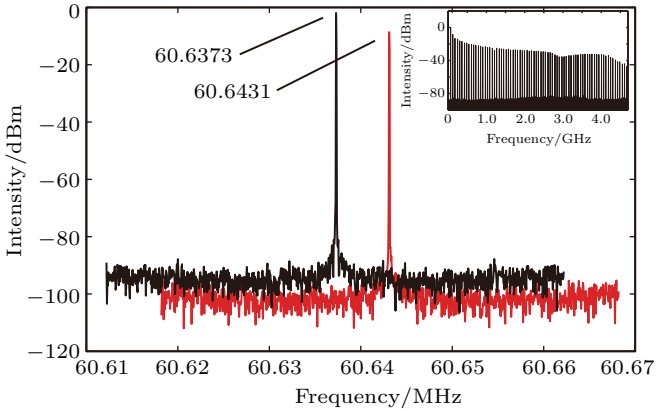


Fig. 3. RF spectra of the PM erbium-doped fiber laser mode-locked at the central wavelengths of 1531.6 nm (red) and 1557.8 nm (black). The inset shows the spectral harmonics at a span of 5 GHz.

The pulse widths of the output laser at 100 mW pump power are measured by a commercial intensity autocorrelator with a scale range of 6.3 ps and a resolution of 5 fs, as shown in Fig. 4. The autocorrelation traces are well fitted by a sech^2 temporal profile. According to the conversion ratio (0.648) between the full width at half maximum (FWHM) pulse width and the FWHM autocorrelation trace width for the hyperbolic secant pulse shape, the FWHM pulse width is equal to 816 fs for the pulses mode-locking at the wavelength of 1531.6 nm, and 402 fs for the pulses mode-locking at the wavelength of 1557.8 nm. Combining with their spectral bandwidths, the calculated time-bandwidth products (TBP) are respectively equal to 0.392 and 0.374, both of which are close to the transform-limit for the sech^2 pulses (0.315). With the pump power increased over 100 mW, pulse

breaking or pulse pair generation for both wavelengths are evidently observed by the autocorrelator. The pulse train of mode-locking at 1531.6 nm is recorded by an oscilloscope (inset in Fig. 4(a)). There is $\sim$ 16.5 ns interval between two adjacent pulses, which is consistent with the measured fundamental frequency of 60.64 MHz by the RF analyzer. The pulse train of mode-locking at 1557.8 nm has the same characteristic (not shown here).

According to the gain spectrum of the erbium-doped fiber, continuous wave or mode-locked laser at 1532 nm is aroused in the higher-loss fiber cavity than longer wavelength laser. So, the aroused nonlinear effects in the fiber cavity of the mode-locked laser at 1532 nm are weaker than the mode-locking laser working at 1558 nm. Therefore, the number of longitudinal-modes evoked by the nonlinear effects of mode-locking at 1532 nm is less than that in the laser of 1558 nm. It means that the spectrum-width of mode-locking at 1532 nm is narrower, and the transform-limit pulse-width is wider relative to that at 1558 nm at the same pump power.

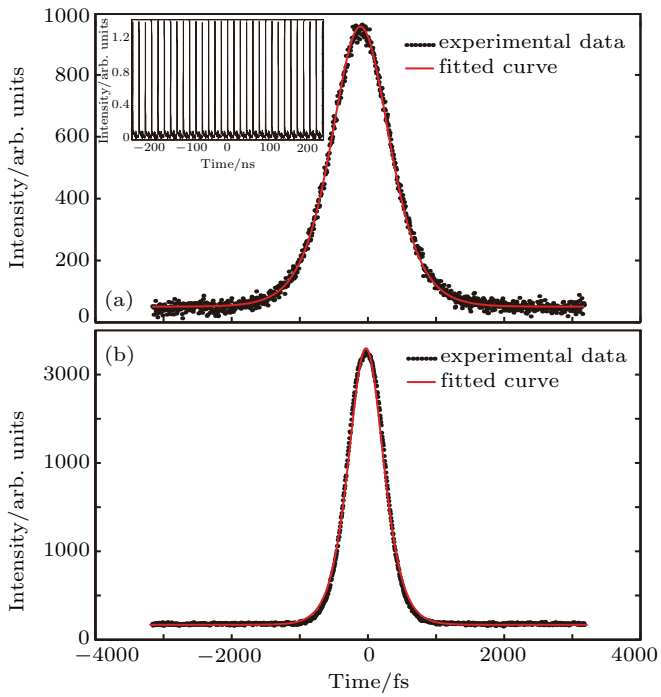


Fig. 4. Autocorrelation traces of all-PM erbium-doped fiber laser pulses mode-locking at the central wavelengths of (a) 1531.6 nm and (b) 1557.8 nm.

Owing to the all-PM fiber cavity, the output laser should be linearly polarized. Measured by a polarization extinction ratio (PER) meter with 0.1 dB resolution for the extinction ratio and $< \pm 0.45^\circ$ accuracy for the polarization angle, the PER of the laser mode-locked at 1531.6 nm is 17.9 dB, and the polarized azimuth angle is $\sim -3.0^\circ$ relative to the slow axis of the fiber. In addition, the PER of the laser mode-locked at 1557.8 nm is 17.3 dB, and the polarized azimuth angle is $\sim 8.3^\circ$. Therefore, both kinds of solitons keep a good degree of linear polarization. But, their polarized azimuth angles are different, which can be attributed to the polarization state of the reflected light influenced by the gold reflector, and induce cavity loss as an important factor.

4. Conclusion

We have demonstrated for the first time, to the best of our knowledge, wavelength-switching solitons in an all-PM erbium-doped ring fiber laser. The mechanism of wavelength switching is qualitatively analyzed by the linear transmission model. Pulses as short as 816 fs of mode-locking at 1531.7 nm and 402 fs of mode-locking at 1557.8 nm are separately generated at $\sim$ 60.64 MHz repetition frequency by adjusting the GSAM. The maximum pulse energies are $\sim$ 40 pJ at the wavelength of 1531.6 nm and $\sim$ 96 pJ at the wavelength of 1557.8 nm while working at the pump power 100 mW. Both of the generated solitons are robust, and have linear polarization with high PER. The wavelength-switchable single-polarization ultrafast laser as an excellent laser source can be applied in the polarization-sensitive measurements and nonlinear frequency conversion processes.

References

[1] Zhang H, Zheng C, Yan P, Gong M, Xiao Q and Zhao Q 2012 *Laser Phys. Lett.* **9** 744
[2] Shen X, Zhang H, Hao H, Li D, Li Q, Yan P and Gong M 2015 *Opt. Commun.* **345** 168
[3] Zhang H, Shen X, Chen D, Zheng C, Yan P and Gong M 2014 *IEEE Photon. Technol. Lett.* **26** 2295
[4] Liu M, Zhang H, Gong M L, Zhao Y J, Cheng W Y, Meng K, Zheng C and Chen Y Z 2014 *Chin. Phys. B* **23** 044214
[5] Lavieja C, Jarabo S, Donagueda M and Sola I J 2013 *Optical Fiber Technol.* **19** 476
[6] Zhu F, Hundertmark H, Kolomenskii A A, Strohaber J, Holzwarth R and Schuessler H A 2013 *Opt. Lett.* **38** 2360
[7] Mollenauer L F and Stolen R H 1984 *Opt. Lett.* **9** 13
[8] Chong A, Renninger W H and Wise F W 2007 *Opt. Lett.* **32** 2408
[9] Cabasse A, Gaponov D, Ndao K, Khadour A, Oudar J and Martel G 2011 *Opt. Lett.* **36** 2620
[10] Ma D, Cai Y, Zhou C, Zong W, Chen L and Zhang Z 2010 *Opt. Lett.* **35** 2858
[11] Kurita T, Yoshida H, Kawashima T and Miyanaga N 2012 *Opt. Lett.* **37** 3972
[12] Okhotnikov O G, Araujo F M and Salcedo J R 1994 *Appl. Phys. Lett.* **65** 2910
[13] Yamashita S and Nishihara M 2001 *IEEE J. Sel. Top. Quant.* **7** 41
[14] Man W S, Tam H Y, Demokan M S, Wai P K A and Tang D Y 2000 *J. Opt. Soc. Am. B* **17** 28
[15] Yan Z, Li X, Tang Y, Shum P P, Yu X, Zhang Y and Wang Q J 2015 *Opt. Express* **23** 4369
[16] Song C, Xu W, Luo Z, Luo A and Chen W 2009 *Opt. Commun.* **282** 4408
[17] Xu H, Lei D, Wen S, Fu X, Zhang J, Shao Y, Zhang L, Zhang H and Fan D 2008 *Opt. Express* **16** 7169
[18] Zhang H, Tang D Y, Wu X, Zhao L M, Bao Q L, Loh K P, Lin B and Tjin S C 2010 *Laser Phys. Lett.* **7** 591
[19] Zhao G Z, Xiao X S, Meng F, Mei J W and Yang C X 2013 *Chin. Phys. B* **22** 104205
[20] Sobon G, Sotor J, Pasternak I, Krajewska A, Strupinski W and Abramski K 2015 *Opt. Express* **23** 9339
[21] Xu J, Wu S, Liu J, Li Y, Ren J, Yang Q and Wang P 2014 *IEEE Photon. Technol. Lett.* **26** 346
[22] Nielsen C K, Ortac B, Schreiber T, Limpert J, Hohmuth R, Richter W and Tunnermann A 2005 *Opt. Express* **13** 9346

[23] Schreiber T, Nielsen C K, Ortac B, Limpert J and Tunnermann A 2006 *Opt. Lett.* **31** 574
[24] Zhang H, Lu S B, Zheng J. Du J, Wen S C, Tang D Y and Loh K P 2014 *Opt. Express* **22** 7249
[25] Lu S B, Miao L L, Guo Z N, Qi X, Zhao C J, Zhang H, Wen S C, Tang D Y and Fan D Y 2015 *Opt. Express* **23** 11183
[26] Sobon G 2015 *Photon. Res.* **3** A56
[27] Davide S, Cafiso D, Ugolotti E, Schmidt A, Petrov V, Griebner U, Agnesi A, Cho W B, Jung B H, Rotermund F, Bae S, Hong B H, Reali G and Pirzio F 2013 *Opt. Lett.* **38** 1745
[28] Chen C J, Wai P K A and Menyuk C R 1992 *Opt. Lett.* **17** 417
[29] Tang D Y, Zhao L M, Zhao B and Liu A Q 2005 *Phys. Rev. A* **72** 043816
[30] Wu J, Tang D Y, Zhao L M and Chan C C 2006 *Phys. Rev. E* **74** 046605
[31] Bass M and Mahajan V N 2010 *Handbook of Optics* (3th Edn.) (New York: McGraw-Hill Professional Press)
[32] Dennis M and Duling I 1994 *IEEE J. Quantum Electron.* **30** 1469
[33] Sobon G, Sotor J and Abramski K M 2012 *Laser Phys. Lett.* **9** 581
[34] Liu X 2011 *Phys. Rev. A* **84** 023835
[35] Zhang S M, Meng Q S and Zhao G Z 2010 *Eur. Phys. J. D* **60** 383